Tests of Models for High-Frequency Seafloor Backscatter

Darrell R. Jackson, Kevin B. Briggs, Kevin L. Williams, and Michael D. Richardson

Abstract— **The interaction of high-frequency sound with the seafloor is inherently a stochastic process. Inversion techniques must, therefore, employ good stochastic models for bottom acoustic scattering. An assortment of physical models for bottom backscattering strength is tested by comparison with scattering strength data obtained at 40 kHz at three shallow water sites spanning a range of sediment types from fine silt to coarse sand. These acoustic data are accompanied by sediment physical property data obtained by core sample analysis and *in situ* probes. In addition, stereo photography was used to measure the power spectrum of bottom relief on centimeter scales. These physical data provided the inputs needed to test the backscatter models, which treat scattering from both the rough sediment–water interface and the sediment volume. For the three sites considered here, the perturbation model for scattering from a slightly rough fluid seafloor performs well. Volume scattering is predicted to be weak except at a site having a layer of methane bubbles.**

I. Introduction

PHYSICALLY based models for acoustic scattering by the seafloor can be inverted to estimate intrinsic seafloor properties such as acoustic impedance, roughness, etc. [1], [2]. These classification "clues" will presumably be only weakly dependent upon nonintrinsic factors such as propagation, pulselength, and transducer directivity and should, therefore, provide a basis for robust seafloor classification algorithms. One approach is to begin with measurement of seafloor scattering strength and to invert for seafloor properties. This requires use of a carefully calibrated acoustic system, but offers the advantage of exploiting a rather well-developed area of seafloor interacting acoustics.

In this paper, several models for seafloor backscattering strength are examined with the classification problem in mind. The models are illustrated using acoustic and physical property data from three experiments conducted under the Coastal Benthic boundary layer (CBBL) Program. Acoustic data were obtained using a circularly scanning sonar deployed on the seafloor and operating at 40 kHz. Sediment physical property data consist of compressional and shear wave speeds, compressional wave attenuation, porosity, roughness spectrum, and vertical correlation lengths of porosity and compressional wave speed. The variance of porosity is directly proportional to the variance of bulk density and, henceforth, references to fluctuations in sediment density will be based on fluctuations in measured porosity [3].

Manuscript received January 19, 1996; revised May 15, 1996.

D. R. Jackson and K. L. Williams are with the Applied Physics Laboratory, University of Washington, Seattle, WA 98105 USA.

K. B. Briggs and M. D. Richardson are with the Naval Research Laboratory, Stennis Space Center, MS 39529-5004 USA.

Publisher Item Identifier S 0364-9059(96)07988-5.

Models to be considered treat both interface scattering due to roughness and volume scattering due to sediment inhomogeneity and gas bubbles. Models for scattering due to interface roughness include first-order perturbation theory for fluid-like sediments [4] and for elastic sediments [5]–[7]. For fluid-like sediments the composite roughness model [8]–[10] is employed and compared to perturbation theory. For scattering from the sediment volume, the first-order fluid perturbation approach [11]–[14] and the bubble scattering model of Tang *et al.* [15] are used.

II. Experimental Methods

Acoustic scattering data and sediment physical property data were acquired at three shallow water sites which will be designated "Eckernförde," "Panama City," and "Key West." Data were acquired in April 1993 at the Eckernförde site (54° 29.5' N; 9° 59.0' E), a shallow bay in the southwestern Baltic Sea. This site had a water depth of 26 m, a silty clay sediment, and a layer of free methane bubbles approximately 1 m below the sediment–water interface. The Panama City experiment was conducted in August 1993 at a site on the West Florida Sand Sheet (29° 41.1' N; 85° 40.7' W) having water of depth 29 m and a coarse-grained sandy sediment mixed with carbonate shell hash. Measurements were made at the Key West site in February 1995. This site was near the Dry Tortugas (24° 36.7' N; 82° 50.7' W) in water of depth 25 m with a sediment consisting of a carbonate sand-silt-clay. The acoustic measurements reported here were obtained using the Benthic Acoustic Measurement System (BAMS) operating at 40 kHz. Other investigators have obtained backscattering data at these sites using other frequencies and geometries [16], [17]. While an extensive set of physical property measurements were made in these experiments [17], [18], only the subset required for the models predicting acoustic backscattering in this paper is discussed here. These data were obtained by core sample analysis, *in situ* probes, and stereo photogrammetry.

A. Sediment Physical Property Measurements

The Eckernförde, Panama City, and Key West experiment sites were characterized by diver-collected cores and stereo photography and found to be relatively uniform within a 1-km^2 area surrounding BAMS. All diver cores were 6.1-cm diameter cylindrical polycarbonate tubes cut to 45-cm lengths and were used to measure compressional wave velocity and attenuation at 400 kHz in 1-cm intervals. Following these

TABLE I
AVERAGE VALUES OF SEDIMENT PHYSICAL PROPERTIES

Site	Grain Size (ϕ)	Compressional Velocity Ratio	Compressional Attenuation (dB/m/kHz)	Shear Velocity (m/s)	Porosity (%)	Density Ratio
Eckernförde	9.9	0.991	0.0707	8.1	86.0	1.18
Panama City	0.8	1.126	0.524	117.0	40.1	1.97
Key West	6.5	1.020	0.321	50.8	56.4	1.72

TABLE II
STATISTICS CHARACTERIZING RANDOM SEAFLOOR PARAMETERS

Site	Compressional Velocity		Porosity		Roughness Spectrum	
	Variance (m^2/s^2)	Vertical Corr. Length (cm)	Variance ($\%^2$)	Vertical Corr. Length (cm)	Slope	Intercept (cm^3)
Eckernförde	3.62	4.63	0.617	2.11	-2.42	0.0003028
Panama City	406.45	1.37	3.90	1.66	-2.12	0.001983
Key West	38.72	4.65	7.25	2.81	-2.29	0.002092

measurements, the cores were cut into 2-cm intervals for which sediment porosity, bulk density and grain size distribution were measured. Velocity, attenuation, porosity, bulk density, and grain size measurements were made using the method described in [10]. Stereo photographs of the sediment–water interface were made with a Photosea 2000M 35-mm stereo camera and a Photosea 1000 100-J underwater strobe joined in a diver-operated module where divers have control over orientation and camera placement. Divers collected series of photographs along 15–30-m-long transects from which selected photographs of the best quality were chosen for analysis. Stereo photographic pairs were analyzed with the Benima stereo comparator described by Briggs [19] to achieve three parallel digitized profiles from each stereo pair. Ten, sixteen, and eight stereo pairs were analyzed from the Eckernförde, Panama City, and Key West sites, respectively.

Measurements of compressional wave velocity and attenuation also were accomplished with the *in situ* sediment acoustic measurement system (ISSAMS) described in Richardson *et al.* [20] and Barbagelata *et al.* [21]. This system provides measurements at 10, 20, and 30 cm below the seafloor and operates at lower frequency (either 38 or 58 kHz, as discussed later) than the core sample apparatus (400 kHz). In addition, ISSAMS was used to measure shear wave velocity at 100–1000 Hz at 30 cm below the seafloor. Average *in situ* compressional wave velocity values were very close to values measured from cores (less than 1% difference). Comparison of *in situ* and core measurements of compressional wave attenuation, however, showed significant departures from linear frequency dependence. The average values of geoacoustic properties in Table I are derived from *in situ* measurements, as these measurements most closely match the frequency of the backscatter measurements (40 kHz). The statistics characterizing fluctuations of compressional wave velocity in Table II are derived from core measurements.

B. Backscattering Measurements

The 40-kHz measurement system (BAMS) [10], [15], [22] operated autonomously for periods of approximately two weeks and was programmed to execute circular scans at rates of 1, 2, and 3 per hour at Eckernförde, Key West, and Panama City, respectively. Each scan consisted of 72 angular steps in 5° intervals, with 5 s between steps. A single planar array was used for both transmission and reception with full beamwidths at half-maximum power of 6.5 and 14.0° in the horizontal and vertical, respectively. The transmitted signal was a linear FM sweep of length 2 ms and bandwidth 2 kHz, centered at 40 kHz with source level 217 dB re 1 μPa @ 1 m. Data were rejected if surface reverberation was significant or if the two-way array vertical directivity was more than 6 dB below maximum. The presence of detectable surface reverberation was inferred from ping–ping correlation [22] and interferometric, or split-beam, bathymetry measurements [15]. These considerations limited scattering strength estimates to a grazing angle range of 5°–20°. Noise was not a factor, as surface reverberation became important at ranges where the signal-to-noise ratio exceeded 20 dB, with the noise floor set by system noise rather than ambient noise. The squared echo envelope was averaged over all 72 pings and this average was used to estimate scattering strength. No matched filtering was used, as the 2-ms pulselength provided sufficient grazing angle resolution. In the grazing angle interval of interest here, resolution is approximately proportional to grazing angle and is about 1° at 10°. An FM sweep is used for the sole purpose of increasing signal bandwidth, which provides more rapidly varying echo envelopes than a pure-tone pulse of equal length, therefore reducing statistical error in backscatter strength estimates. Assuming Gaussian statistics for the echo, and further assuming that all 72 pings comprising one scan come from a statistically homogeneous region of seafloor, the theoretical standard deviation of the resulting scattering strength estimate is 0.25 dB. This error is outweighed by systematic errors in calibration, which are conservatively estimated to be 2 dB.

III. SEDIMENT PHYSICAL PROPERTY DATA

Tables I and II summarize the physical property data used to provide inputs for the backscattering models to be investigated. While the focus in the present paper is on the forward problem, it is useful to realize that, for the inverse problem, the parameters in these tables would be the outputs of an ideal inversion. This point of view serves to delineate the regime that is open to the models under consideration. Figs. 1–3 display profiles of sediment compressional wave velocity and attenuation, porosity, and mean grain size obtained by analysis of core samples from the three sites. The grain size and density ratios given in Table I were obtained by averaging these data over the entire core depth and over all core samples. The density ratio was determined from the average values for sediment porosity, water density and grain density [10]. The compressional wave velocity and attenuation data in Figs. 1–3 were obtained at 400 kHz. The compressional velocity and attenuation data in Table I, as well as the shear

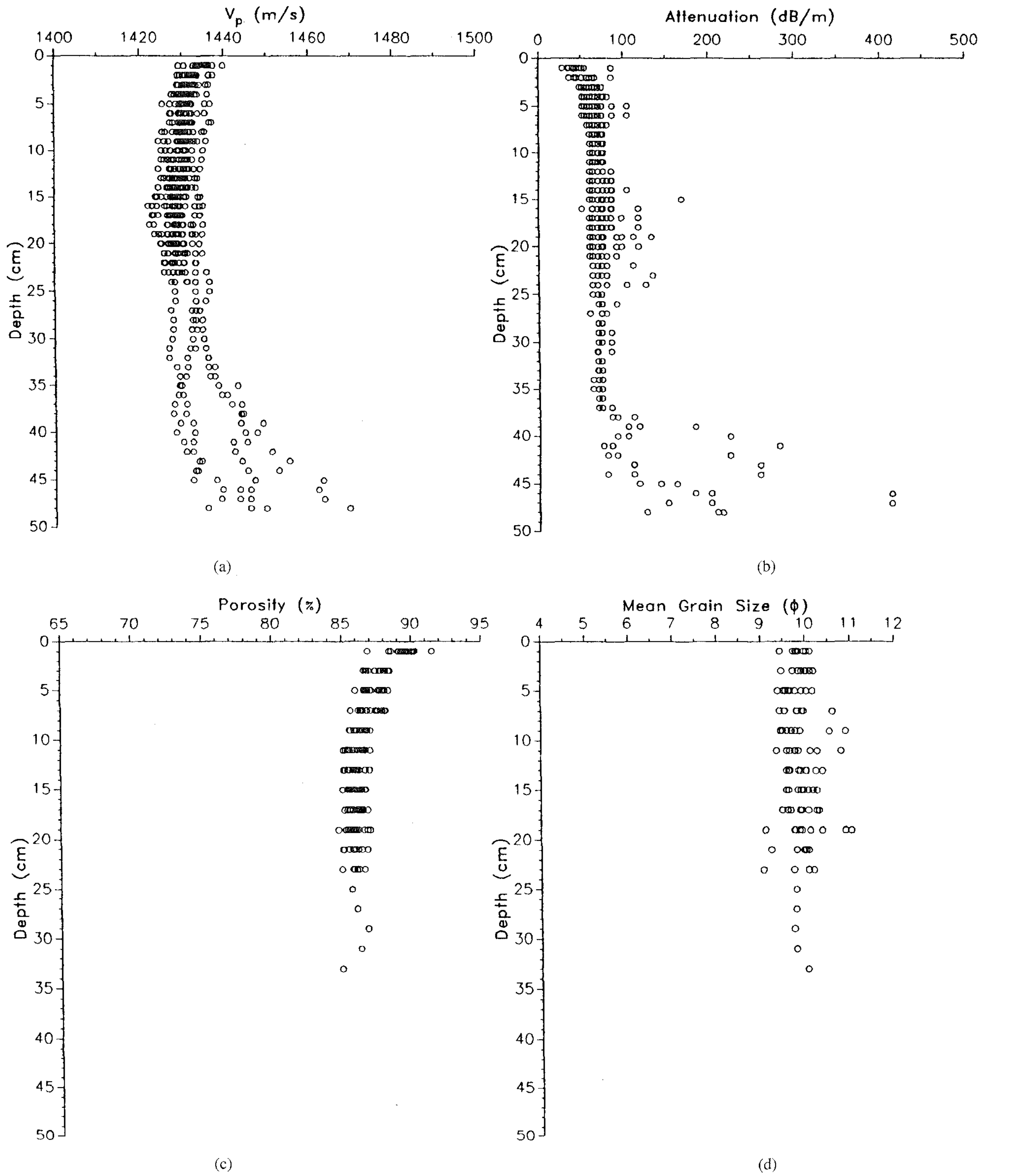

Fig. 1. Profiles of (a) compressional wave velocity, (b) compressional wave attenuation, (c) porosity, and (d) mean grain size determined by analysis of core samples from the Eckernförde site.

wave velocities, however, were measured using ISSAMS. The compressional velocity and attenuation measurements were made at a frequency of 38 kHz at the Key West site and at 58 kHz at the other two sites. Measurement of geoacoustic properties at frequencies near those used in acoustic scattering measurements ameliorates problems associated with velocity dispersion and the choice of a mathematical relationship between attenuation and frequency [23]. All ratios in Table I are quotients of the sediment parameter divided by the corresponding parameter for the water immediately above the seafloor.

The average parameters in Table I govern acoustic propagation in the sediment. In principle, inversion of the models to be considered here will permit acoustic measurement of these

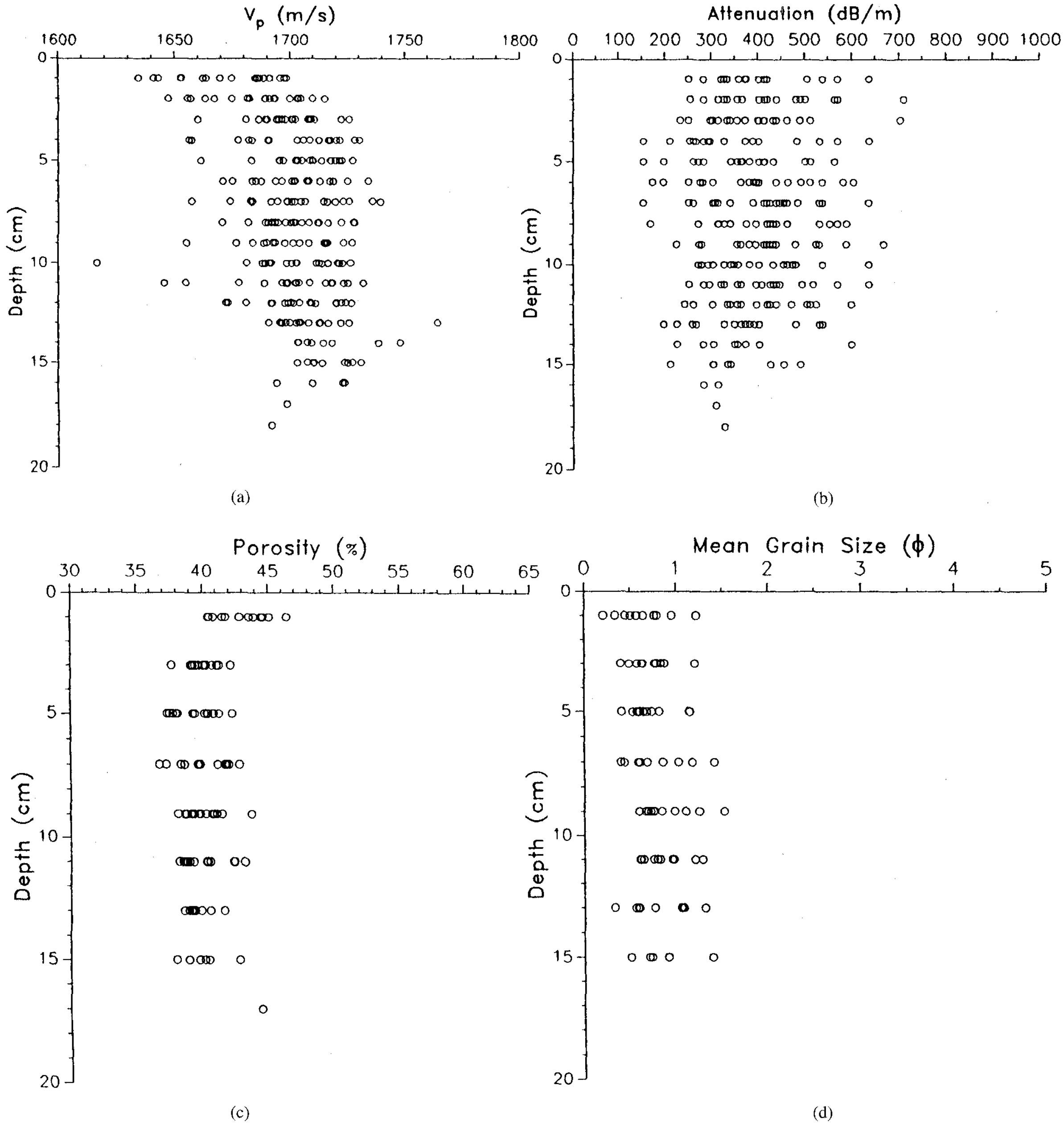

Fig. 2. Profiles of (a) compressional wave velocity, (b) compressional wave attenuation, (c) porosity, and (d) mean grain size determined by analysis of core samples from the Panama City site.

parameters. As noted later, dependence of the models upon these parameters is typically not very strong, consequently other means may be needed to constrain these parameters. Nonetheless, in the forward problem, accurate values for these parameters are essential in rigorous model testing.

The scattering models depend strongly upon parameters characterizing fluctuations in velocity and density and roughness of the water-sediment interface. Table II lists various statistics characterizing these random variables. The covariances of compressional velocity and porosity were estimated by a procedure [3] which takes account of the short length of the core sample records. First, a least-squares linear regression was used for each core to remove any trend due to gradients in porosity or sound velocity. The residuals from each core were then tested to determine if they could be considered as uncorrelated "white noise" as opposed to the alternative hypothesis, namely, that the residuals are generated by a positively correlated first-order autoregressive process. The latter process has an exponential correlation function which is of intrinsic interest as it is sometimes assumed in scattering models [12], [13] and has been investigated in more detail by Briggs [3]. However, other authors have found the power-law form to be both convenient and consistent with acoustic data [10], [24], [26]–[28], so the issue as to the best statistical

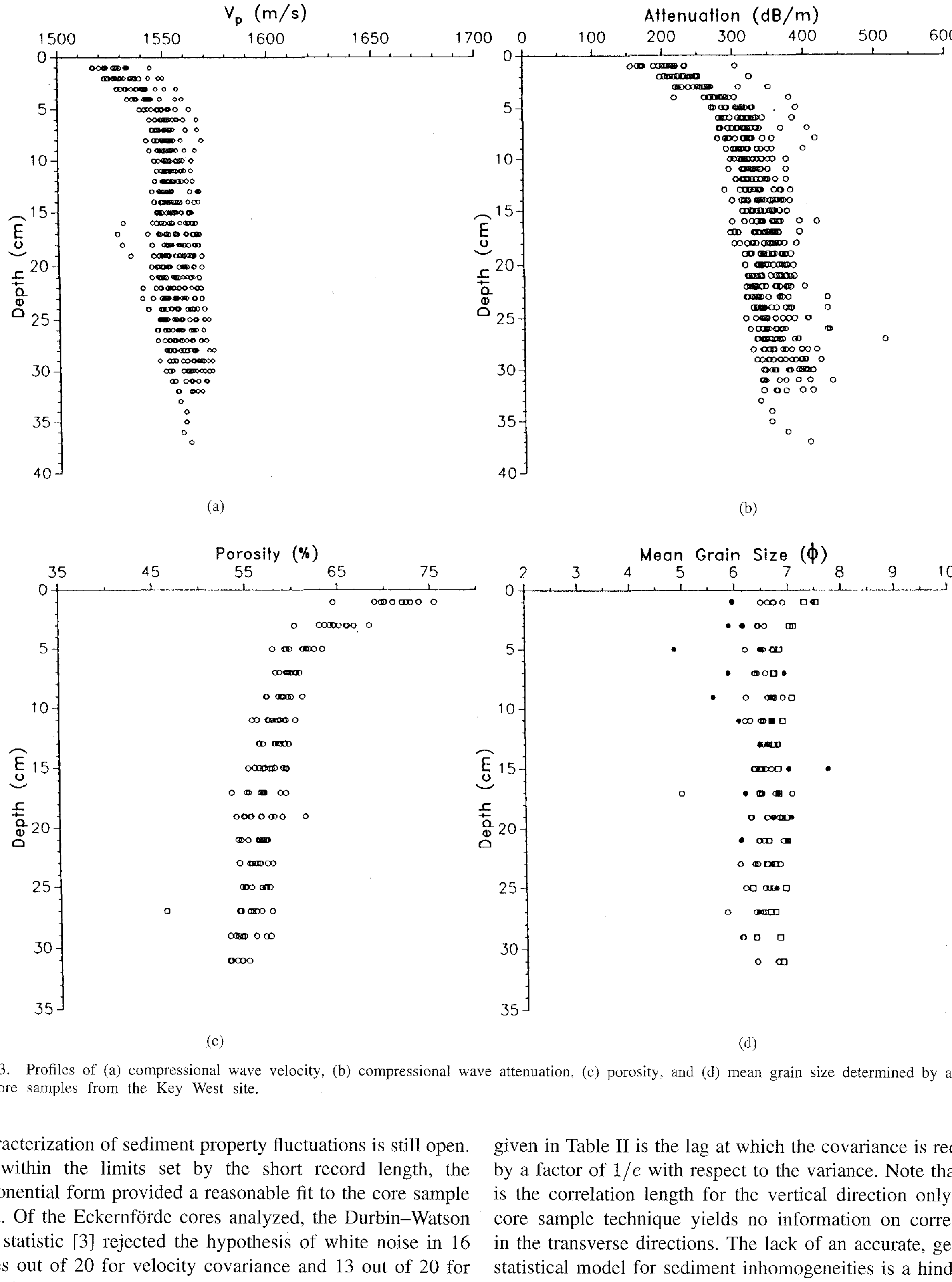

Fig. 3. Profiles of (a) compressional wave velocity, (b) compressional wave attenuation, (c) porosity, and (d) mean grain size determined by analysis of core samples from the Key West site.

characterization of sediment property fluctuations is still open. To within the limits set by the short record length, the exponential form provided a reasonable fit to the core sample data. Of the Eckernförde cores analyzed, the Durbin–Watson test statistic [3] rejected the hypothesis of white noise in 16 cases out of 20 for velocity covariance and 13 out of 20 for porosity covariance. The corresponding numbers for Panama City and Key West are: (13 of 19, 5 of 14) and (19 of 19, 11 of 13). Finally, these estimates were averaged over those cores providing both velocity and porosity covariance estimates and fitted by an exponential. The correlation length given in Table II is the lag at which the covariance is reduced by a factor of $1/e$ with respect to the variance. Note that this is the correlation length for the vertical direction only. The core sample technique yields no information on correlation in the transverse directions. The lack of an accurate, general, statistical model for sediment inhomogeneities is a hindrance to inversion that will only be removed with further research. For the present, the isotropic exponential model is employed primarily because of its simplicity.

The roughness power spectrum for each site (Figs. 4–6) was estimated from three parallel, digitized, profiles from

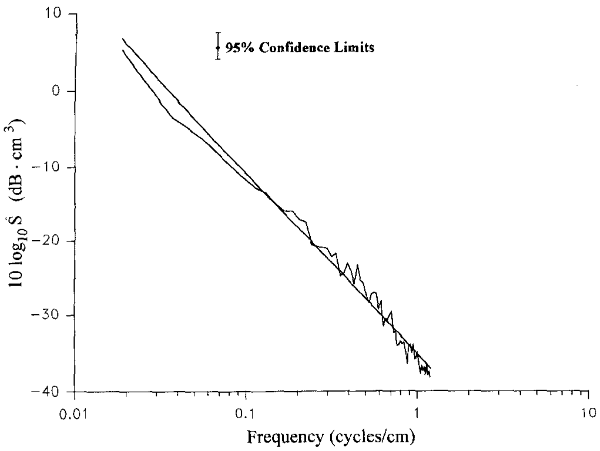

Fig. 4. Roughness spectrum determined by analysis of stereo photographs from the Eckernförde site, with power-law regression fit and 95% statistical confidence limits shown.

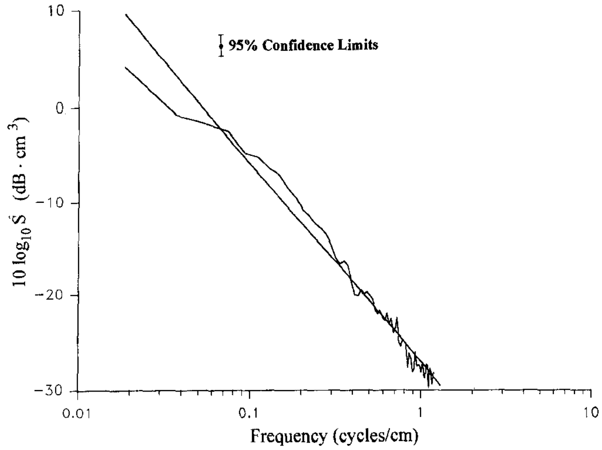

Fig. 5. Roughness spectrum determined by analysis of stereo photographs from the Panama City site, with power–law regression fit and 95% statistical confidence limits shown.

each stereo photographic pair and averaged over all stereo pairs. The slope and intercept given in Table II were obtained by regression fits to the spectral density [19], with spatial frequency in cycles/centimeters. The spectra span nearly two decades in spatial frequency, with the upper frequency determined by the sampling interval of 0.42 cm. Thus the shortest roughness wavelength that is measured is 0.84 cm. The roughness wavelengths of primary interest are of the order of the Bragg wavelength and longer (see the following discussion of models for roughness scattering) which is approximately one-half the acoustic wavelength, or about 2 cm. Thus the measured roughness spectra comfortably include the spatial frequency range employed by the models to be tested. As Figs. 4–6 show, the power–law fits appear quite reasonable in comparison to the 95% statistical confidence limits. The spectra are one-dimensional and two-sided such that the integral over positive spatial frequency yields one-half the variance of seafloor roughness in square centimeters. Inversions for roughness statistics are on firmer ground than those for volume inhomogeneity, as the power–law spectral form is well documented as providing reasonable fits to data from numerous sites [10], [19].

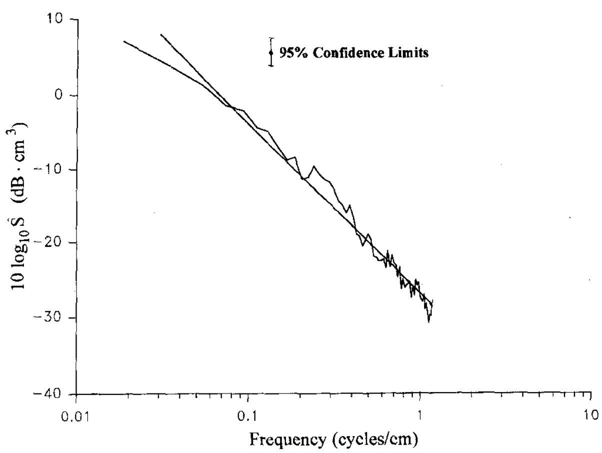

Fig. 6. Roughness spectrum determined by analysis of stereo photographs from the Key West site, with power–law regression fit and 95% statistical confidence limits shown.

IV. Backscattering Data

Fig. 7 compares backscattering strength measured as a function of grazing angle for the three sites. The Panama City and Key West data show rather typical grazing angle dependence, with a monotonic increase in scattering strength as grazing angle increases and with the most rapid increase at small angles. While the Eckernförde data exhibit a markedly different, nonmonotonic angular dependence, Tang *et al.* [15], have shown that this dependence is an experimental artifact, therefore it is not a useful classification clue. This point will be discussed in the model-data comparisons to follow. The backscattering strength data from the three sites are rather similar in level, despite the fact that the sites are quite different in their physical properties. Such similarity is common and

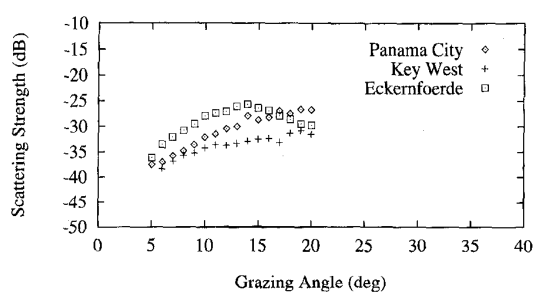

Fig. 7. A comparison of 40-kHz backscattering strength data from the Panama City, Key West, and Eckernförde sites.

shallow-angle backscattering strength. Additional information is needed to remove ambiguity, such as a wider range of grazing angles and/or frequency dependence.

The acoustic data set is too small to allow rigorous tests of inversion based upon scattering strength. Consequently, models to the classification problem, pointing out advantages and pitfalls whenever possible. This effort is greatly facilitated by the unusually complete set of ground-truth physical data available for the three experiments.

V. Models for Backscattering Strength

Five separate models for backscattering strength will be defined, relying on the literature for detail. Three models for scattering from interface roughness will be considered, including perturbation models for viscous fluids and elastic solids. These models will be compared to the composite roughness model with the sediment treated as a viscous fluid. The fluid sediment model will also be used in treating scattering from sediment volume inhomogeneities in the perturbation approximation. For the Eckernförde site, a model for scattering from gas bubbles will be considered.

While the models considered here are well represented in the literature, they do not cover the entire spectrum. For example, other authors have used the Kirchhoff [8], [29] and small-slope [30] approximations. Chotiros and colleagues have argued for the importance of porosity (Biot slow waves) [31], [32], grain scattering [33], and microscopic gas bubble [34], [35] effects. Obviously, model inversion will give useful results only to the extent that the model represents the true scattering mechanism. Thus it is worth reiterating the two primary assumptions made in the present work, that the sediment can be modeled as a fluid (from an acoustic point of view), and that scattering is due either to the roughness of the water–sediment interface or inhomogeneities of the sediment. In the latter case, the inhomogeneities must be due to either relatively gentle modulations of physical properties (as examplified by the core sample data presented earlier) or to a layer of strong scatterers (as at the Eckernförde site).

With respect to the fluid assumption, the discussion to follow makes a strong case against the importance of shear effects. While the issue of Biot effects is not settled, the present approach is supported by several examples of successful application of the fluid assumption to the forward problem [3], [8]–[10]. The assumption of scattering due to gentle modulations of sediment properties will undoubtedly fail at very high frequencies for which the wavelength approaches the grain size, so that the sediment can no longer be treated as a continuum. In the present paper, the wavelength is about 3.75 cm, and the largest mean grain size is about 0.5 mm. Consequently, it seems likely that the continuum assumption is valid. A breakdown of the assumption of gentle modulation may occur in sediments having numerous solid inclusions, such as shell, but no systematic study has been made of this effect.

Table III gives values for the input parameters required by the models under consideration. These were either obtained directly from the tabular values given earlier or derived from them. These parameters will be defined in the course of the following discussion of the models. Inversion for a given parameter will be most accurate when the model output depends strongly on that parameter. Qualitative comments on the sensitivity to various parameters will be offered in the later discussion of model–data comparisons, but a detailed, quantitative study is beyond the scope of this paper.

TABLE III
Input Parameters Used in Model–Data Comparisions

Site	Compressional Velocity Ratio ν	Compressional Loss Parameter δ	Shear Velocity (m/s) V_s	Density Ratio ρ	Density Spectral Exponent γ_3	Density Spectral Strength (cm³) w_3
Eckernförde	0.991	0.00186	8.1	1.18	4.0	3.52×10^{-6}
Panama City	1.126	0.0166	117.0	1.97	4.0	1.61×10^{-5}
Key West	1.020	0.00915	50.8	1.72	4.0	2.41×10^{-5}

TABLE IV. Table III continued. Input parameters used in model-data comparisons.

Site	Density Correlation Length (cm) l_c	Compressibility Fluctuation Ratio μ	Roughness Spectral Exponent γ_2	Roughness Spectral Strength (cm⁴) w_2	Water Sound Velocity m/s c
Eckernförde	2.11	-0.69	3.42	0.00231	1448
Panama City	1.66	-2.44	3.12	0.00849	1532
Key West	2.81	-1.31	3.29	0.0122	1525

A. Perturbation Approximation for Roughness Scattering

For the fluid sediment model, the perturbation treatments used by recent authors are derivatives of the result given by Kuo [4]. The particular form employed here has been discussed by Mourad and Jackson [9] and Jackson and Briggs [10]. The latter reference elaborates the definitions given in (5.1)–(5.3).

The acoustic properties of the sediment are determined by the compressional velocity ratio ν, the compressional loss parameter δ, and the density ratio ρ. The loss parameter is related to the compressional wave attenuation coefficient α as follows:

$$\delta = \frac{\alpha \nu c \ln(10)}{40\pi f}. \tag{5.1}$$

The ratio of attenuation to frequency (α/f) is given in Table I in units of dB/m/kHz. With these units, the water sound speed c appearing in (5.1) must be in units of m/ms in order to obtain the correct value for δ.

Interface roughness is characterized by a two-dimensional spectrum that is assumed isotropic, with a power–law dependence on wavenumber:

$$W(k_x, k_y) = \frac{w_2}{h_0^{\gamma_2}(k_x^2 + k_y^2)^{\gamma_2/2}}. \tag{5.2}$$

The exponent γ_2 is the absolute value of the spectral slope of Table II plus unity and $h_0 = 1$ cm is a trivial parameter used to balance units in this and following equations. The spectral strength w_2 is related to the spectral intercept ϕ_1 of Table II as follows:

$$w_2 = (2\pi)^{\gamma_2 - 2}\phi_1 h_0 \frac{\Gamma(\gamma_2/2)}{\sqrt{\pi}\Gamma[(\gamma_2 - 1)/2]} \tag{5.3}$$

where Γ is the gamma function.

The parameters defined here are inserted in the expressions of [9] or [10] to obtain backscattering strength as a function of grazing angle and frequency. The scattering cross section in this model is proportional to the roughness spectrum evaluated at the Bragg wavenumber, $2k\cos\theta$. Since wavenumber is proportional to frequency, the frequency dependence of scattering can in principle, be used to trace out the roughness spectrum. The wavenumber dependence of the spectrum is governed by the parameter γ_2, with scattering strength increasing with frequency at a rate of $3(4-\gamma_2)$ dB/octave. For the spectral exponents of Table III, this is a slow increase, less than 3 dB/octave.

Although no rigorous tests have been made of the mathematical accuracy of the perturbation approximation in the context of scattering from rough, lossy fluids, exact computations [36], [27] for backscattering from a pressure–release rough interface show that the perturbation approximation is accurate provided the rms surface roughness h satisfies

$$kh < 0.5 \tag{5.4}$$

where k is the acoustic wavenumber in water. Application of this inequality to the present case is problematic because the power–law spectrum yields infinite rms roughness if it is assumed to apply over all spatial frequencies. While this is surely not the case, it is not clear which wave number cutoff is appropriate for determining h. The composite roughness model to be discussed later takes this cutoff to be of the order of the acoustic wavenumber.

The perturbation approximation has been applied to elastic sediments by Kuperman and Schmidt [5] and Dacol and Berman [6]. The formulation used here is equivalent to that of Essen [7] who treated the lossy, or elastic case. Details of this approach are given by Ivakin and Jackson [39] who provide expressions in a form analogous to those of the fluid case. This model requires all the parameters of the fluid perturbation model plus two additional parameters: the velocity and attenuation of shear waves in the sediment. As the shear velocity becomes much smaller than the sound velocity in water, this model produces backscattering strength values that are nearly equal to those of the fluid model. This will be the case in the present examples, for which the largest shear wave velocity (for the Panama City site) is only 117 m/s. In this regime, the model prediction is insensitive to shear attenuation, so the lack of measured values for this parameter is not a problem.

B. Composite Roughness Approximation

The composite roughness approximation has been successfully applied to scattering from the sea surface [40] and this success motivates its use for scattering from the seafloor. This approximation begins with the perturbation result and introduces corrections to account for the effects of the large-scale components of seafloor roughness. The correction scheme of Jackson *et al* [8] as modified by Mourad and Jackson [9] will be used. Without going into details, it can be noted that "large-scale" roughness is essentially defined as that part of the seafloor relief corresponding to wavenumbers smaller than the acoustic wavenumber. This approximation uses the same set of input parameters as the fluid perturbation approximation, and the roughness spectral parameters are used to compute the rms slope of the large-scale roughness. This slope parameter is used in expressions that correct for the effects of local tipping of the seafloor and shadowing. As will be seen, these corrections are negligible except for small grazing angles. Although Thorsos [37] has shown that these composite roughness corrections are accurate for sea surface scattering when they are small, there is reason to suspect these corrections in the case of seafloor scattering. The difference in the two cases lies in the smaller spectral exponent for seafloor roughness as compared to sea-surface roughness (typically 3.0 to 3.6 for seafloor roughness versus 4 for sea-surface roughness). In the case of seafloor scattering, this causes the bulk of the large-scale slope to be due to roughness wavelengths only slightly longer than the acoustic wavelength, calling into question the "large-scale" approximation used in the corrections. Jackson and Briggs [10] experienced difficulty in applying the composite roughness approximation to data from a sandy site, although this difficulty had another cause: unrealistic extrapolation of a high-slope spectrum to low wavenumbers. These issues await resolution by mathematical tests of the composite-roughness approximation using numerically intensive "exact" calculations, along the lines used to test approximations for sea-surface scattering [37].

C. Perturbation Approximation for Sediment Volume Scattering

Scattering by sediment inhomogeneities is recognized as a major contributor to seafloor backscattering [8], [10]–[14], [25], [28], [38]. Following the approach of Ivakin and Lysanov [11], recent theoretical work has employed perturbation theory for fluid sediments [12], [13], [28], [38] although Ivakin [25] has treated elastic sediments and Yelton and Chotiros [33] have developed a one-dimensional model for multiple scattering in porous sediments. Here, the fluid model will be used in the form presented by Jackson [24], but this formulation is equivalent to that used by authors cited above. Because the published account of Jackson's formulation is not readily available, the relevant expressions are summarized here. Sound absorption usually limits sediment volume scattering to a thin layer immediately below the sediment–water interface. This makes it possible to describe sediment volume scattering in terms of an equivalent interface scattering strength given by the decibel equivalent of following dimensionless interface scattering cross section [10]:

$$\sigma = \frac{\sigma_v|1-R(\theta)^2|^2\sin^2\theta}{4k|P(\theta)|^2\,\mathrm{Im}\,[P(\theta)]} \tag{5.5}$$

where

$$P(\theta) = \sqrt{\kappa^2 - \cos^2\theta} \tag{5.6}$$

and

$$\kappa = \frac{1+i\delta}{\nu}. \tag{5.7}$$

The reflection coefficient, $R(\theta)$, is used in the form:

$$R(\theta) = \frac{y-1}{y+1} \tag{5.8}$$

with

$$y = \frac{\rho \sin\theta}{P(\theta)}. \tag{5.9}$$

In (5.5),

$$\sigma_v = (\pi/2)k^4|\mu\kappa^2 - \cos^2\theta - P^2(\theta)|^2 W_{\rho\rho}(\Delta k) \tag{5.10}$$

is the volume scattering strength in the perturbation approximation. The density fluctuation spectrum appearing in (5.10) will be taken in the form [26]:

$$W_{\rho\rho}(\boldsymbol{k}) = \frac{w_3}{h_0^{\gamma_3}(k^2 + 1/l_c^2)^{\gamma_3/2}}. \tag{5.11}$$

In (5.10), the spectrum is evaluated at the Bragg wavenumber:

$$\Delta k = 2k[\cos^2\theta + (\mathrm{Re}\,[P(\theta)])^2]^{1/2}. \tag{5.12}$$

With reference to (5.11) and Table III, w_3 is the density spectral strength, γ_3 is the density spectral exponent, and l_c is the correlation length. The argument of the density spectrum is a three-dimensional wavevector $\boldsymbol{k}$ but isotropy is assumed so that the spectrum depends only upon the magnitude k of $\boldsymbol{k}$. This assumption is implicit in Hines [12] model–data comparisons, but Lyons *et al.* [13] find that anisotropy must be invoked to obtain a good fit to backscatter data at 6.5 kHz. Yamamoto's [27] tomographic measurements indicate substantial anisotropy on scales of several meters and larger. Isotropy is assumed here mainly as a reasonable means of applying the available one-dimensional fluctuation data to this three-dimensional problem. The density fluctuation spectrum is defined so that its integral over all $\boldsymbol{k}$ (positive and negative) is equal to the variance of the density ratio divided by the square of the mean density ratio. Thus the spectral strength is related to the variance of the density ratio σ_ρ^2 as follows:

$$w_3 = \frac{h_0^{\gamma_3}(\sigma_\rho^2/\rho^2)l_c^{3-\gamma_3}\Gamma(\gamma_3/2)}{\pi^{3/2}\Gamma(\gamma_3/2 - 3/2)}. \tag{5.13}$$

The core data available for the sites of interest provided profiles of porosity versus depth, from which an exponential covariance was estimated as described earlier. A Fourier transform of the exponential covariance can be used to show that the corresponding spectrum is a special case of (5.11) with

$$\gamma_3 = 4 \tag{5.14}$$

and l_c equal to the correlation length of the exponential covariance, that is, the lag at which the covariance is equal to the variance divided by e. In this case, (5.13) simplifies to

$$w_3 = \frac{h_0^4\sigma_\rho^2}{\pi^2 l_c \rho^2}. \tag{5.15}$$

Using the relation between porosity and density ratio, the variance of the density ratio is related to the variance of porosity σ_p^2 (Table II) the average porosity p (Table I) and the average density ratio ρ (Table I) as follows:

$$\sigma_\rho^2 = \frac{\sigma_p^2}{100^2}\frac{(1-\rho)^2}{(1-p/100)^2}. \tag{5.16}$$

This expression was used to scale the porosity variance to obtain the density ratio variance appearing in (5.15). This completes the correspondence between the parameters of Tables I and II and the density spectral parameters of Table III.

Generally, scattering in an inhomogeneous fluid is caused by fluctuations in both density and sound velocity, so the density spectrum is insufficient for predictions of scattering. For the special case of backscattering, fluctuations in the product of density and sound velocity (the acoustic impedance) govern scattering. In the small perturbation approximation used here, the fluctuation of interest is thus the sum of the normalized (divided by mean) density and velocity fluctuations. It will be assumed that velocity fluctuations are, at every point in the sediment, proportional to density fluctuations with a position-independent proportionality factor. Equivalently, Lyons *et al.* [13] and Jackson [24] assume that compressibility fluctuations are proportional to density fluctuations. Defining the parameter μ as the ratio of normalized compressibility to normalized density fluctuations [see (5.10)] the values for μ given in Table III are obtained by using the known relation between velocity, density and compressibility. This leads to the following expression in terms of the standard deviations of density ratio and compressional velocity:

$$\mu = -1 \mp \frac{2\sigma_v \rho}{\sigma_\rho c \nu}. \tag{5.17}$$

In (5.17), c is the sound speed for the water immediately above the seafloor and σ_v is the square root of the compressional velocity variance given in Table II. The choice of sign in (5.17) depends upon whether sediment compressional wave velocity and density fluctuations are positively or negatively correlated. Most often, one expects compressional wave velocity in sediments to increase as density increases, that is, compressional wave velocity and density are positively correlated, and the $(-)$ sign should be used in (5.17). This was the case for the Panama City and Key West sites. For very fine sediments, however, compressional wave velocity may decrease as density increases, and the $(+)$ sign should be used. The data compilation of Richardson and Briggs [23] suggests this should occur when porosity is greater than about 80% or density is less than about 1.4 g/cm^3. Accordingly, the $(+)$ sign was used for the Eckernförde site. The best means of determining this sign is to estimate the sign of the crosscorrelation as part of the processing of core samples, but this was not done. In fact, the rare cases of sign reversal occur when $|2\sigma_v\rho/\sigma_\rho c\nu| \ll 1$, so incorrect use of the $(-)$ sign should not be of great consequence.

D. Single Scattering Model for Gas Bubbles in Sediment

Tang *et al.* [15] found that a relatively simple model for scattering from bubbles could account for the 40-kHz backscattering data from the Eckernförde site. This model will be adapted to the present context so that it can be compared directly with the other models of interest. The present approach proceeds in two stages. In the first stage, a sonar-equation model is developed for the received echo intensity time series. In the second stage, this time series is inverted to extract interface scattering strength. Details of this approach will be omitted as this is an elementary application of Snell's law and the sonar equation.

A two-stage approach is necessary because, as Tang *et al.* point out, the scatterers are not situated on the sediment-water interface as assumed in the inversion, but are at an appreciable depth (approximately 1 m) beneath it. Thus the inversion used to obtain the results of Fig. 12 is incorrect, and these errors must be included in any model that is to be compared with the inverted data. Following Tang *et al*, the bubble layer is represented by a thin layer of scatterers, with scattering strength determined by bubble size, shape, and density. The received time series is readily obtained by considering propagation from the transducer through the refractive interface, through the lossy sediment to the scattering layer, and back. This approach is a refinement of that of Tang *et al.*, who did not include the effects of refraction upon transmission loss and ensonified area. This leads to slight differences in the two approaches at small grazing angles as will be noted later.

VI. Model-Data Comparisons

Although a true test of the usefulness of backscattering models for sea-floor classification would involve inversions to estimate model parameters, a less ambitious approach will be followed, comparing the models with backscatter data using measured input parameters. Such an approach is warranted as solution of the direct problem must precede solution of the inverse problem. As appropriate, conclusions will be drawn concerning the likely accuracy of inversions. Because the sites are so different in their physical attributes, they will be treated separately, beginning with the simplest case (Panama City) and then moving to increasingly problematic environments.

A. Panama City

Fig. 8 compares the roughness perturbation, composite roughness and volume perturbation models with the backscatter data from the Panama City site. The roughness perturbation model matches the data quite well, while the composite roughness model predicts scattering strengths higher than measured by about 2–4 dB for small grazing angles (5–8°). In this instance, the composite roughness corrections to the perturbation approximation appear to be of doubtful utility. This result is not surprising in light of the comments made earlier about the likely accuracy of these corrections. The volume scattering prediction lies more than 15 dB below the data, showing rather definitely that volume scattering is unimportant for this coarse sand sediment. Errors in estimation of the density fluctuation spectrum are too small to negate this conclusion.

Treatment of this coarse sand as a lossy fluid may seem questionable, as it is not a fluid in the ordinary sense and does support shear waves. Fig. 9 compares the lossy fluid

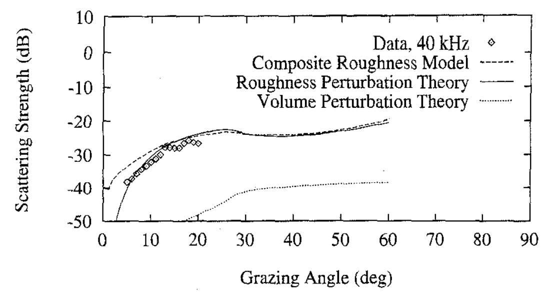

Fig. 8. Backscattering strength data and model predictions for the Panama City site using parameters averaged over core depth.

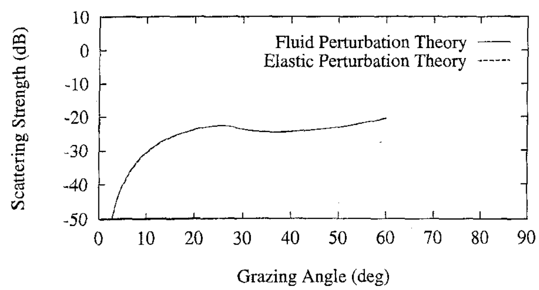

Fig. 9. Comparison of fluid and elastic roughness perturbation models for the Panama City site.

and elastic roughness perturbation models using the measured shear velocity (117 m/s) and assuming no shear loss. There is no appreciable difference in the two model predictions, and this result is unchanged when shear losses of the order given by Hamilton [41] are introduced. This matches the conclusion reached by Ivakin and Jackson [39] that sands can be treated as acoustic fluids even though they are shear-supporting solids in the rheological sense. This leaves open the question as to whether a Biot treatment is necessary to include poro-elastic effects in the scattering model.

Based on the results at hand, the roughness perturbation model provides the best prediction of backscattering for this coarse sand seafloor. If sediment mass density and compressional wave velocity can be estimated or measured by other means, inversion of the perturbation model will provide a good estimate of the roughness spectrum at the Bragg wavenumber, as noted earlier. Backscattering measurements at different frequencies can be used to trace out the spectrum at different wavenumbers. As backscattering cross section is proportional to the spectrum in this model, errors in measuring backscattering strength translate directly into errors in estimation of the roughness spectrum; for example, a 3-dB error corresponds to a factor-of-two error in spectrum estimation. With regard to other model parameters, the scattering cross section in the perturbation approximation has a slow and complicated dependence upon sediment mass density and compressional wave attenuation, hence these parameters are difficult to estimate in this context. The cross section depends strongly upon compressional wave velocity, provided it exceeds the water sound speed. In this case, the backscattering cross section has a slight "bump" in the grazing angle domain [8] (see Fig. 8) providing a feature that might be used to determine

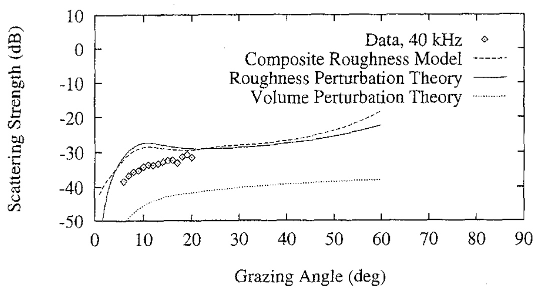

Fig. 10. Backscattering strength data and model predictions for the Key West site using parameters averaged over core depth.

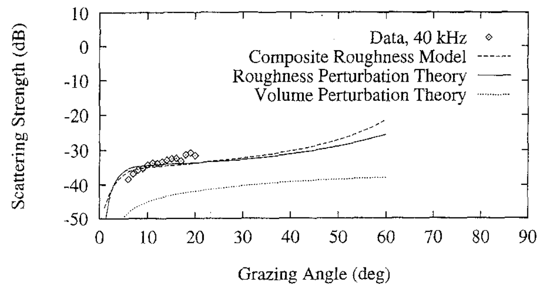

Fig. 11. Backscattering strength data and model predictions for the Key West site using surficial parameters.

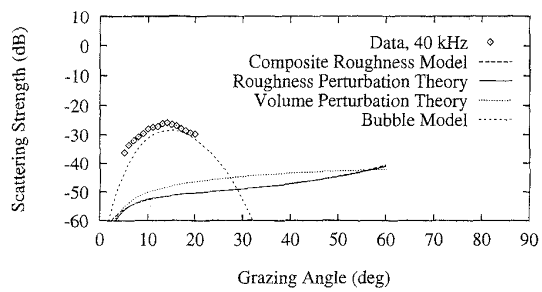

Fig. 12. Backscattering strength data and model predictions for the Eckernförde site using parameters averaged over core depth.

compressional wave velocity. Unfortunately, the predicted bump is seldom large compared to experimental errors, also, volume scattering may mask the bump.

B. Key West

As Fig. 10 shows, the roughness scattering strength prediction falls above the Key West data by several decibels, while the volume scattering prediction falls well below the data. The bump in the curves for both the roughness perturbation and composite roughness models (due to the critical angle effect) would not normally be expected in such a fine sediment. In fact, the profiles of physical properties for this site (Fig. 3) show that the sediment is quite waterlike near the interface. The transition from these waterlike properties to the less porous and acoustically "harder" sediment represented by the average parameters of Table I occurs over the upper 6 cm. The best means of treating such gradients would be to use a generalized perturbation formalism [42], [43]. This requires numerical computation of the plane-wave reflection coefficient including gradients in density and in compressional wave velocity and attenuation. Instead, the simpler procedure of using surficial values for these parameters [9], [10] will be used. Thus, the compressional wave velocity and density ratios given in Table 1 will be reduced to 1.0 and 1.475, respectively. The loss parameter will not be changed, as the value in the table is deduced from *in situ* measurements at 38 kHz and is likely to be more accurate than a value scaled from the core data at 400 kHz. Fig. 11 shows that the model-data fit is greatly improved by this modification. This sea floor is smoother than that at the Panama City site, consequently the composite roughness and perturbation models provide nearly the same prediction.

Sediments with strong gradients such at this present a challenging inversion problem. At least one gradient parameter must be estimated in addition to the present set of model inputs, consequently additional data beyond scattering strength at a single frequency and at low grazing angles are needed to determine this larger set of unknowns. Such data may be provided by backscattering measurements at vertical incidence, and at several different frequencies.

C. Eckernförde

The Eckernförde sediment is extremely soft and waterlike. As a result of this lack of acoustic contrast, roughness scattering predictions fall well below the data, as seen in Fig. 12. The interface is quite smooth, as indicated by the small value of the spectral strength w_2. Perturbation and composite roughness models therefore produce very similar predictions. Volume perturbation predictions also fall well below the data, indicating that scattering is due to some process not included in these models. As shown by Tang *et al.* [15], the methane bubble layer observed at this site accounts for the observed backscattering. The modified version of their model provides the approximately parabolic curve seen in Fig. 12 when the parameters of Table III are combined with the bubble layer scattering strength (-10.8 dB) obtained by fitting the acoustic data [15] and subsequently supported using available data on bubbles at this site [44]. Tang *et al.* obtained the best fit by decreasing sediment acoustic absorption by 0.4 dB/m relative to the measured value. In the present case, this alteration still leaves a difference of about 2 dB between the model and data. This remaining difference is a result of the refinements that have been included in the present form of the model and indicates that some of the other model inputs require slight adjustment to achieve a good fit. As the measurement errors are approximately 2 dB, such tweaking is probably not justified.

The Eckernförde data show an unusual downturn as grazing angle exceeds 13°. This occurs because the scatterers are not on the sediment–water interface as assumed when extracting scattering strength from the data. At the larger grazing angles, the true arrival angle of the acoustic energy is appreciably steeper than the presumed angle, and this results in undercorrection for array directivity. Thus, the downturn is not an intrinsic feature of the sea floor at this site but is dependent upon the properties of the measurement system and is, therefore, not a robust classification clue. It can be concluded that scattering strength measurements do not provide a useful means of classifying buried bubble layers. The interferometric bathymetry method exploited by Tang *et al.* is better suited to this purpose.

VII. Conclusion

The model/data comparisons presented here answer several questions relating to seafloor classification and raise several more. For hard sand seafloors, roughness perturbation theory offers an attractive model for inversion purposes. This model may also find application to softer sediments, although strong gradients such as those appearing at the Key West site should be treated by using a generalized version of perturbation theory. The composite roughness model does not appear to offer any significant advantage over the simpler perturbation model. None of the examples considered here provided a convincing test of the volume perturbation model, owing to the low levels of predicted volume scattering relative to roughness scattering. It is clear, however, that progress is needed in characterizing sediment inhomogeneities. Uncertainties as to suitable forms for covariances and spectra must be resolved, and one-dimensional measurements must be replaced by measurements capable of quantifying anisotropy on centimeter scales. Nevertheless, the predicted scattering dependence is sensitive to spectral parameters in a manner analogous to roughness scattering, so the prospects for inversion are good. Finally, cross correlations between sediment properties (e.g., porosity and compressional wave velocity) must be determined. Volume scattering from dense aggregations of deeply buried bubbles, as at the Eckernförde site, requires a completely different approach and cannot be treated as an equivalent interface scattering process.

Acknowledgment

The data reported here were the result of the efforts of many CBBL participants at NRL-SSC, The Applied Physics Laboratory of the University of Washington, and Forschunganstalt der Bundeswehr für Wasserschall- und Geophysik, Kiel, Germany. Thanks are also due the officers and crew of the vessels that supported the Eckernförde, Panama City, and Key West CBBL experiments.

References

[1] C. de Moustier and D. Alexandrou, "Angular dependence of 12 kHz seafloor acoustic backscatter," *J. Acoust. Soc. Amer.*, vol. 90, pp. 522–531, July 1991.

[2] H. Matsumoto, R. P. Dziak, and C. G. Fox, "Estimation of seafloor microtopographic roughness through modeling of acoustic backscatter data recorded by multibeam sonar systems," *J. Acoust. Soc. Amer.*, vol. 94, pp. 2776–2787, Nov. 1993.

[3] K. B. Briggs, "High-frequency acoustic scattering from sediment interface roughness and volume inhomogeneities," Naval Research Lab. NRL/FR/7431-94-9617, Dec. 1994.

[4] E. Y. T. Kuo, "Wave transmission and scattering at irregular interfaces," *J. Acoust. Soc. Amer.*, vol. 36, pp. 2135–2142, Nov. 1964.

[5] W. A. Kuperman and H. Schmidt, "Rough surface elastic wave scattering in a horizontally stratified ocean," *J. Acoust. Soc. Amer.*, vol. 79, pp. 1767–1777, June 1986.

[6] D. K. Dacol and D. H. Berman, "Sound scattering from a randomly rough fluid-solid interface," *J. Acoust. Soc. Amer*, vol. 84, pp. 292–302, July 1988.

[7] H. H. Essen, "Scattering from a rough sedimental seafloor containing shear and layering," *J. Acoust. Soc. Amer.*, vol. 95, pp. 1299–1310, Mar. 1994.

[8] D. R. Jackson, D. P. Winebrenner, and A. Ishimaru, "Application of the composite roughness model to high-frequency bottom backscattering," *J. Acoust. Soc. Amer.*, vol. 79, pp. 1410–1422, May 1986.

[9] P. D. Mourad and D. R. Jackson, "High frequency sonar equation models for bottom backscatter and forward loss," in *Proc. OCEANS '89*, vol. 4, Sept. 1989, pp. 1168–1175.

[10] D. R. Jackson and K. B. Briggs, "High-frequency bottom backscattering: roughness vs. sediment volume scattering," *J. Acoust. Soc. Amer.*, vol. 92, pp. 962–977, Aug. 1992.

[11] A. N. Ivakin and Yu. P. Lysanov, "Theory of underwater sound scattering by random inhomogeneities of the bottom," *Sov. Phys. Acoust.*, vol. 27, pp. 61–64, 1981.

[12] P. C. Hines, "Theoretical model of acoustic backscattering from a smooth seabed," *J. Acoust. Soc. Amer.*, vol. 88, pp. 325–334, July 1990.

[13] A. P. Lyons, A. L. Anderson, and F. S. Dwan, "Acoustic scattering from the seafloor: Modeling and data comparison," *J. Acoust. Soc. Amer.*, vol. 95, pp. 2441–2451, May 1994.

[14] D. Tang, "Acoustic wave scattering from a random ocean bottom," Ph.D. dissertation, Massachusetts Inst. Technology, and Woods Hole Oceanographic Institution, 1991.

[15] D. Tang, G. Lin, D. R. Jackson, and K. L. Williams, "Analysis of high-frequency bottom and subbottom backscattering for two distinct shallow-water environments," *J. Acoust. Soc. Amer.*, vol. 96, pp. 2930–2936, Nov. 1994.

[16] M. D. Richardson, "Investigating the coastal benthic boundary layer," *EOS*, vol. 75, pp. 201–206, 1994.

[17] S. G. Tooma and M. D. Richardson, "The Key West campaign, university, government laboratory, international effort focuses on coastal benthic boundary layer, combining basic, applied programs," *Sea Technology*, vol. 36, pp. 17–25, June 1990.

[18] M. D. Richardson and W. R. Bryant, "Benthic boundary layer processes in coastal environments: An introduction," *Geo Marine Lett.*, vol. 16, pp. 133–139, Aug. 1996.

[19] K. B. Briggs, "Microtopographical roughness of shallow-water continental shelves," *IEEE J. Oceanic Eng.*, vol. 14, pp. 360–367, Oct. 1989.

[20] M. D. Richardson, S. R. Griffin, and F. B. Gross, "ISSAMS: An in-situ sediment acoustic measurement system," in *Proc. Int. Conf. on Underwater Acoustics*, Univ. of New South Wales, Sydney, Australian Acoustical Society, pp. 104–106.

[21] A. Barbagelata, M. Richardson, B. Miaschi, E. Muzi, P. Guerrini, L. Troiano, and T. Akal, "ISSAMS: An in situ sediment acoustic measurement system," in *Shear Waves in Marine Sediments*, J. M. Hovem, M. D. Richardson, and R. D. Stoll, Eds. Dordrecht, The Netherlands: Kluwer, 1991, pp. 305–312.

[22] J. G. Dworski and D. R. Jackson, "Spatial and temporal variation of acoustic backscatter in the STRESS experiment," *J. Continental Shelf Res.*, vol. 14, pp. 1221–1237, Aug. 1994.

[23] M. D. Richardson and K. B. Briggs, "On the use of acoustic impedance values to determine sediment properties," in *Acoustic Classification and Mapping of the Seabed*, N. G. Pace and D. N. Langhorne, Eds. Bath, U.K.: Institute of Acoustics, 1993, pp. 15–25.

[24] D. R. Jackson, "Models for scattering from the sea bed," *Proc. Inst. Acoust.*, vol. 16, pp. 161–169, Dec. 1994.

[25] A. N. Ivakin, "Sound scattering by inhomogeneities of an elastic half space," *Soviet Physics, Acoustics*, vol. 36, pp. 377–380, 1990.

[26] ——, "Modeling of sound scattering by the sea floor," *J. de Physique III*, vol. 4, pp. C5-1095–C5-1098, May 1994.

[27] T. Yamamoto, "Velocity variabilities and other physical properties of marine sediments measured by crosswell acoustic tomography," *J. Acoust. Soc. Amer.*, vol. 98, pp. 2235–2248, Oct. 1995.

[28] ——, "Acoustic scattering in the ocean from velocity and density fluctuations in the sediments," *J. Acoust. Soc. Amer.*, vol. 99, pp. 866–879, Feb. 1996.

[29] C. S. Clay and H. Medwin, *Acoustical Oceanography: Principles and Applications*. New York: Wiley-Interscience, 1977, pp. 502–526.

[30] T. Yang and S. L. Broschat, "Acoustic scattering from a fluid–elastic–solid interface using the small slope approximation," *J. Acoust. Soc. Amer.*, vol. 96, pp. 1796–1803, Sept. 1994.

[31] F. A. Boyle and N. P. Chotiros, "Experimental detection of a slow acoustic wave in sediment at shallow grazing angles," *J. Acoust. Soc. Amer.*, vol. 91, pp. 2615–2619, May 1992.

[32] N. P. Chotiros, "Biot model of sound propagation in water-saturated sand," *J. Acoust. Soc. Amer.*, vol. 97, pp. 199–210, Jan. 1995.

[33] D. J. Yelton and N. P. Chotiros, "New multiple scatter model of the ocean sediment," *J. Acoust. Soc. Amer.*, vol. 97, pt. 2, p. 3387, May 1995.

[34] F. A. Boyle and N. P. Chotiros, "A model for acoustic backscatter from muddy sediments," *J. Acoust. Soc. Amer.*, vol. 98, pp. 525–530, July 1995.

[35] F. A. Boyle and N. P. Chotiros, "A model for high-frequency acoustic backscatter from gas bubbles in sandy sediments at shallow grazing angles," *J. Acoust. Soc. Amer.*, vol. 98, pp. 531–541, July 1995.

[36] E. I. Thorsos and D. R. Jackson, "The validity of the perturbation approximation for rough surface scattering using a Gaussian roughness spectrum," *J. Acoust. Soc. Amer.*, vol. 86, pp. 261–277, July 1989.

[37] E. I. Thorsos, "Acoustic scattering from a "Pierson-Moskowitz" sea surface," *J. Acoust. Soc. Amer.*, vol. 88, pp. 335–349, July 1990.

[38] N. G. Pace "Low frequency acoustic backscatter from the sea bed," Proc. Inst. Acoust. vol. 16, pp. 181–188, Dec. 1994.

[39] A. N. Ivakin and D. R. Jackson, "Effects of shear elasticity on sea bed scattering: Numerical examples," to be published.

[40] S. T. McDaniel and A. D. Gorman, "Acoustic and Radar sea surface backscatter," *J. Geophys. Res.*, vol. 87, pp. 4127–4136, May 1982.

[41] E. L. Hamilton, "Attenuation of shear waves in marine sediments," *J. Acoust. Soc. Amer.*, vol. 60, pp. 334–338, Aug. 1976.

[42] A. N. Ivakin, "Sound scattering by rough interfaces of layered media," in *Proc. Third Int. Congress on Air- and Structural-Borne Sound and Vibration*, pp. 1563–1570, June 1994.

[43] J. E. Moe and D. R. Jackson, "First-order perturbation solution for rough surface scattering cross section including the effects of gradients," *J. Acoust. Soc. Amer.*, vol. 96, pp. 1748–1754, Sept. 1994.

[44] D. Tang, Modeling high-frequency acoustic backscattering from gas voids buried in sediments," *Geo Marine Lett.*, vol. 16, pp. 261–265, Aug. 1996.

Darrell R. Jackson received B.S., and the Ph.D. degrees from the University of Washington, in 1960, 1963, and 1966, respectively, all in electrical engineering.

From 1960 to 1967, he worked at The Boeing Company as a Research Engineer. He joined the Electrical Engineering faculty of the University of Massachusetts, Amherst, in 1968 and returned to graduate school in 1972, receiving the Ph.D. degree in physics from Caltech in 1977. Since 1976, he has been with the Applied Physics Laboratory of the University of Washington where his research is centered on acoustical oceanography and underwater acoustics with emphasis on acoustic interaction with the sea floor. He is currently Chair of the Acoustical Oceanography Technical Committee of the Acoustical Society of America.

Dr. Jackson is a fellow of the Acoustical Society of America and a member of the American Geophysical Union.

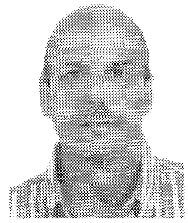

Kevin B. Briggs received the B.S. degree in biology from Florida Atlantic University, Boca Raton, in 1975, the M.S. degree in zoology from the University of Georgia, Athens, in 1978, and the Ph.D. degree in marine geology and geophysics from the University of Miami, Rosenstiel School of Marine and Atmospheric Science, Miami, FL, in 1994.

He began working at the Naval Ocean Research and Development Activity, now part of the Naval Research Laboratory (NRL), at the Stennis Space Center in Mississippi in 1979, where he was involved in research on the effects of environmental processes on sediment geoacoustic properties. He has participated in many shallow-water high-frequency experiments as an investigator of geoacoustic and roughness properties of the seafloor and is currently engaged in research on characterization of sediment interface roughness and volume inhomogeneity for high-frequency acoustic models.

Dr. Briggs is a member of the Acoustical Society of America and the American Geophysical Union.

Kevin L. Williams received the B.S., M.S., and Ph.D. degrees in physics from Washington State University, Washington, in 1979, 1983, and 1985 respectively.

He worked at the Naval Coastal Systems Center in Panama City, FL, from 1985 to 1988 where his primary focus was in acoustic scattering from finite bodies and propagation into ocean sediments. In 1988, he moved to the Applied Physics Laboratory, University of Washington, where he has worked in the area of high frequency environmental acoustics, studying scattering and propagation in Arctic ice and ocean sediments. He has over 30 published articles on acoustic scattering.

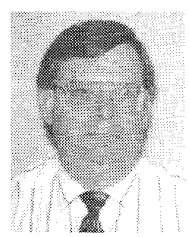

Michael D. Richardson received the B.S. degree in oceanography from University of Washington in 1967, the M.S. degree in marine science from the College of William and Mary in 1971, and the Ph.D. degree in oceanography from Oregon State University in 1976.

Dr. Richardson began working at the Naval Research and Development Activity, now part of the Naval Research Laboratory (NRL), located at the Stennis Space Center, MS, in 1977. Except for a five-year assignment as principal scientist at NATO's SACLANTCEN in La Spezia, Italy (185-89); he has worked at NRL as a senior scientist and is currently head of the Geoacoustic and Geotechnique section in the Marine Geosciences Division. He is also the chief scientist of Office of Naval Research sponsored Coastal Benthic Boundary Layer program. Research interests include the effects of biological and hydrodynamic processes on sediment structure, behavior, and physical properties near the sediment-water interface both in shallow-water coastal regions and in the deep-sea.

Dr. Richardson is a member of the Acoustical Society of America, American Geophysical Union, European Geophysical Society and Sigma Xi.